

# AXIAL ALIGNMENT AND THERMAL GROWTH EFFECTS ON TURBOMACHINERY TRAINS WITH DOUBLE-HELICAL GEARING

by

**Thom Eldridge**

**Manager of Aero/Thermodynamics Engineering Design**

**Dresser-Rand Company**

**Olean, New York**

**Greg Elliott**

**Senior Project Engineer**

**Ed Martin**

**Project Engineer**

**Lufkin Industries**

**Lufkin, Texas**

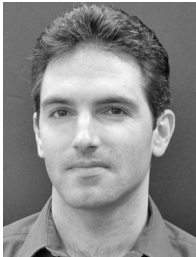
and

**M. Shukri Hitam**

**Turbomachinery Group Superintendent**

**Petronas Carigali**

**Terengganu, Malaysia**



*Thom Eldridge is Manager of the Aero/Thermodynamics Engineering Design Department at Dresser-Rand Company in Olean, New York. His previous responsibilities as supervisor of the Rotordynamics Group included managing the analysis of turbomachinery and guiding rotordynamic development activities. Before joining Dresser-Rand, he worked on bearing development, turbomachinery modeling, data acquisition systems, and high-temperature*

*transducer design as a senior engineer and project team leader for Bently Nevada.*

*Mr. Eldridge received a B.S. and an M.S. degree (Mechanical Engineering, 1991, 1994) from Washington State University, and an MBA degree (2002) from the University of Nevada. He is a registered Professional Engineer in the State of California. Mr. Eldridge holds two patents and has written several papers on damper seals and hydrostatic bearing applications.*



*Greg Elliott is a Senior Project Engineer in the Power Transmission Division of Lufkin Industries in Lufkin, Texas. His primary responsibilities include product development and standardization, as well as engineering systems development. He also supports Lufkin engineering groups with finite element analysis, fatigue analysis, and other applications of engineering mechanics in machinery design and problem solving. Before joining Lufkin,*

*he worked in research and teaching at Texas A&M University.*

*Mr. Elliott received a B.S. and an M.S. degree (Agricultural Engineering, 1982, 1990) from Texas A&M University.*



*Ed Martin is a Project Engineer in the Power Transmission Division of Lufkin Industries, in Lufkin, Texas. He is currently responsible for the engineering functions of Lufkin's high-speed gear product line. He also performs lateral rotordynamic analyses and has been heavily involved in troubleshooting gear vibration, noise, and temperature problems during his 14-year career with Lufkin.*

*Mr. Martin received a B.S. degree (Mechanical Engineering, 1990) from the University of Texas at Austin. He has given numerous presentations on gearing principles and vibration issues, and is also an active member of the AGMA 6011 committee on high-speed helical gearing.*

---

## ABSTRACT

Turbomachinery shafting and casings typically experience axial growth during thermal transients occurring at startup, shutdown, and changes of load. This growth does not usually present difficulties during operation. However, this paper discusses four recent turbomachinery trains that experienced radial subsynchronous vibration resulting from axial misalignment. In each example, the train included a gearbox with a double-helical gearset that presented a lateral vibration response at system torsional critical frequencies while operating at low load. Thermal growth resulted in axial misalignment that produced a "zero-backlash" condition when one helix contacted on the back side of the teeth. Data collected with an axial displacement probe verified the appearance of lateral subsynchronous vibration was associated with excessive axial misalignment of the gearset. Data are presented from these experiences, including a discussion of other vibration phenomena that could be mistaken for this behavior. Finally, design and analysis recommendations are provided for preventing such occurrences.

## INTRODUCTION

The authors have encountered several instances of unacceptable gearbox lateral vibration arising from forces external to the gearbox caused by axial misalignment. Most of the lessons learned from these experiences build upon previous findings (Zirkelback, 1979; Mancuso, 1986; Carter, et al., 1994). However, most emphasis has been placed on parallel or angular alignment problems. Although axial alignment problems may occur less frequently, the delays and expense caused by such problems make it worthwhile to share this information with others in the rotating equipment community. This paper presents necessary background, examples, and recommendations for problem diagnosis and prevention.

### Helical Gearing Background

Parallel-shaft, double-helical gearing is widely used in high-speed, high-power turbomachinery applications. In these applications, double-helical designs usually are the best choice because of their high power density, smooth meshing, reduced thermal distortion, high-energy efficiency, and high reliability. The term “double-helical” refers to the use of two sets of helical teeth arranged with opposing helix directions. Figures 1 and 2 show typical double-helical gearsets used in turbomachinery trains. Figures 3 and 4 illustrate basic gear terminology (Dudley, 1984; Townsend, 1991).

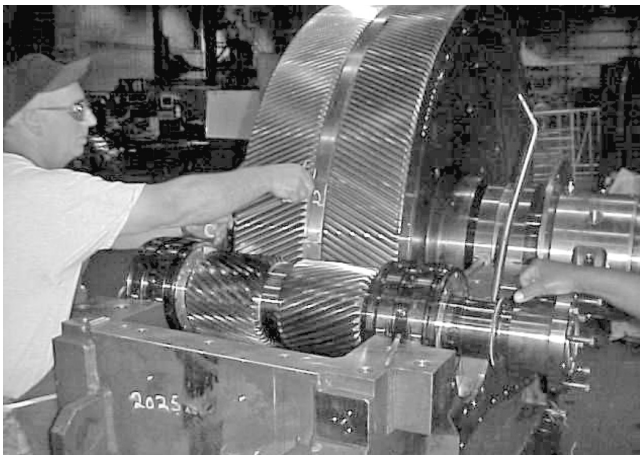


Figure 1. Double-Helical Gearset Used in a Motor–Compressor Drive.

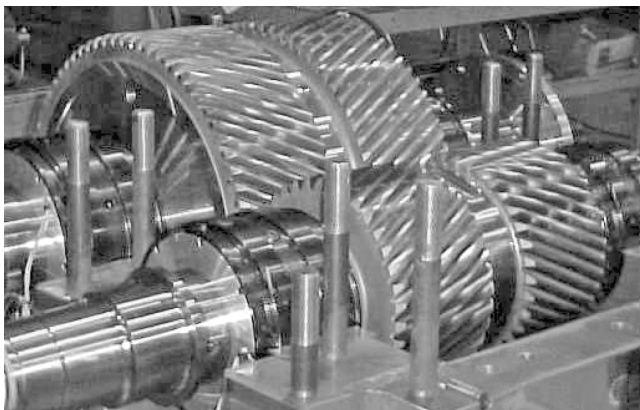


Figure 2. Double-Helical Gearset Used in a Gas Turbine–Compressor Drive.

Axial thrust induced by gear mesh force is a characteristic of helical gearing that is particularly significant to the topic of axial alignment. The axial mesh force of a set of helical gear teeth is calculated (Dudley, 1984) as:

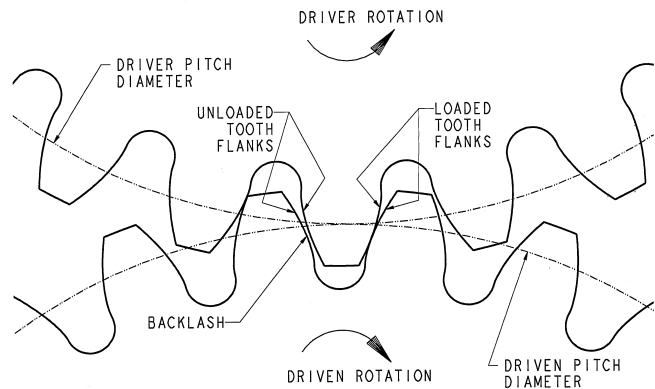


Figure 3. Gear Terminology.

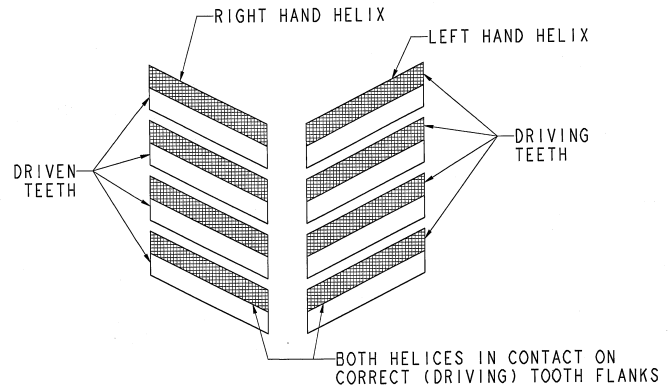


Figure 4. Gear Mesh Centered.

$$F_{MESH} = (2T / D_P) * \tan(H) \quad (1)$$

where:

- $F_{MESH}$  = Mesh centering force (lbf)
- $T$  = Transmitted torque (inch-lbf), per helix
- $D_P$  = Pitch diameter (inch)
- $H$  = Helix angle (degrees)

The force can be quite strong. For example, in a typical double-helical gearset with a 12 inch (305 mm) pitch diameter and a 28-degree helix angle transmitting 40,000 horsepower (30,000 kW) from a gas turbine at 5000 rpm to a centrifugal compressor at 10,000 rpm, each helix generates an axial force of about 11,000 lbf (49,000 N). When applying the formula, one must use the transmitted torque and pitch diameter together for the same element. When applying it to double-helical gearing, the actual transmitted torque per helix should be used.

Under normal circumstances, the mesh forces act equally on each element in opposite directions. This causes the axial mesh forces to cancel internally within a double-helical gearset. Canceling the axial force eliminates the need for high-capacity thrust bearings that would otherwise be required in the gearbox to absorb the axial mesh force. Typically, a gearbox with double-helical gearing will have one thrust bearing on the low-speed gear. If the connected equipment permits, a double-helical gearbox may have no thrust bearing. Additional information on helical gearing can be found in numerous references (Dudley, 1984; Drago, 1988; *Dudley's Gear Handbook*, 1991).

### Double-Helical Mesh Axial Alignment

The axial alignment problem discussed in this paper pertains to double-helical gearing. If the external axial forces on the gear elements are less than the mesh centering force, the mesh holds the pinion centered on the gear as shown in Figure 4. If the external axial force is zero, then the torque load on each helix is equal.

Backlash (clearance) between the teeth is provided in the gearset to avoid contact of the nondriving (back) sides of the teeth. In double-helical gearing, backlash can be defined in the circumferential and axial directions. Circumferential backlash is illustrated in Figure 3. The axial backlash is equal to the circumferential backlash divided by the tangent of the tooth helix angle. For typical turbomachinery applications, a small double-helical gearset might have 0.015 inch (0.4 mm) circumferential backlash and 0.028 inch (0.7 mm) axial. Large gearsets may have three or four times those amounts. However, it is important to note that the axial backlash so defined includes the total potential axial displacement of the pinion relative to the gear in both directions. The pinion can move off center of the gear in each direction only by a distance equal to half the axial backlash. For a gearset with 0.028 inch (0.4 mm) of axial backlash, the teeth will bind if one attempts to shift the pinion more than 0.014 inch (0.4 mm) off center in either direction relative to the gear. This is illustrated in Figures 4, 5, and 6.

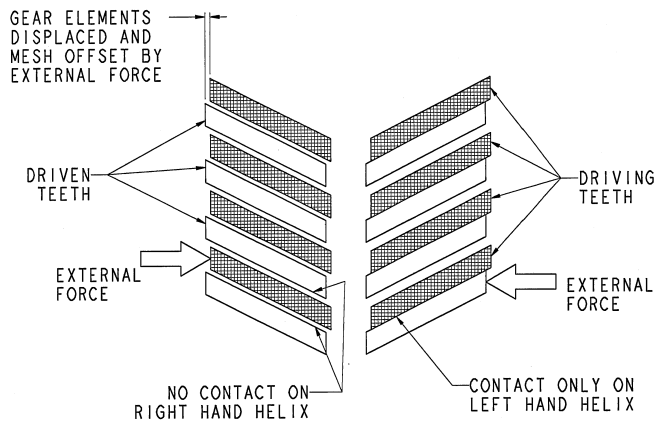


Figure 5. Gear Mesh Offset Axially.

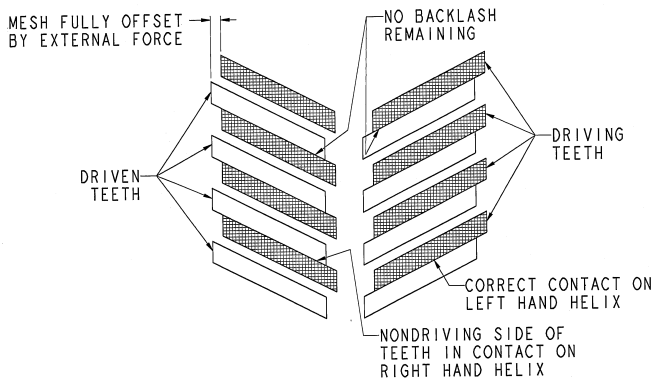


Figure 6. Gear Mesh Bound Axially.

In turbomachinery trains, often there will be axial forces caused by axial misalignment, thermal effects, thrust bearings, magnetic centering forces from electrical machines, gravity loads during ship pitch, and so on. As previously described, when an external axial force is applied to the double-helical gearset, it offsets part of the axial mesh force. This causes no harm (or axial displacement) if the external force is small compared to the axial mesh force. That is typically the condition while service torque is applied. If the external force is larger than the mesh axial force, the two meshing gear elements can be pushed axially out of proper engagement as shown in Figure 5. This is most likely to occur when torque load is small, as may be encountered with a no-load string test, standby operation of a generator set, or during startup or shutdown transients.

If the source of the external force reaches equilibrium with the axial mesh force, the gearset may run satisfactorily on one helix (as

in Figure 5). This can occur, for example, when a flexible coupling is involved. If axial backlash is sufficient, the coupling axial force decreases as the pinion moves off center until the coupling axial force equals the mesh axial force. In Figure 5, the backlash is sufficient to maintain clearance at the nondriving sides of the teeth and permit the gearset to run smoothly. Note that when the gearset is running on one helix, the total transmitted torque is carried on that helix alone. Typically, when service torque load is applied, the mesh force increases and the gearset centers itself axially. If the external axial force is significant compared to the axial mesh force at service torque, it may cause unequal loading of the helices and decrease load carrying capacity.

If the external force is greater than the axial mesh force, it will push the gearset into a bound condition as shown in Figure 6. In this state there is still contact on the normally loaded (driving) tooth flanks on one helix. On the other helix there is contact on the back (nondriving) flanks of the teeth (which should not normally be in contact). Running with contact on the driving side of one helix and the nondriving side of the other helix is similar to operating with zero backlash. It is well known that high-speed, high-power gearing should not be run without backlash (Dudley, 1984).

#### Quantifying External Axial Forces

As previously identified, external axial forces can originate from a number of sources. Frequently such a force is generated by the axial displacement of a flexible element coupling (in compression or tension). Many turbomachinery trains include either a disc or diaphragm coupling between the gearbox and the connected equipment shaft ends. Axial displacement of coupling flexible elements can originate from prestretch of the coupling, axial alignment inaccuracies, and from thermal growth of equipment (both steady-state and transient conditions). The main purpose of coupling prestretch is to cancel out the steady-state thermal growth of the coupling and shaft ends. In this paper, transient thermal growth and axial alignment errors are shown to result in excess axial forces that are capable of forcing the pinion out of center with the gear of a minimally loaded gearset.

A simple estimate of the axial force generated by a flexible element coupling can be obtained through the axial stiffness of the coupling:

$$F_{AXIAL} = D_{SE} * K \quad (2)$$

where:

$F_{AXIAL}$  = External axial force (lbf)

$D_{SE}$  = Relative displacement of shaft ends attached to the coupling (inch)

$K$  = Axial stiffness of the flexible element coupling (lbf/in)

The expected displacement of the shaft ends can be calculated. Commonly it will be a function of axial alignment error and thermal growth. Evaluation of the mesh centering force [Equation (1)] defines an upper bound to the allowable external axial force [Equation (2)]. This establishes a maximum allowable error in axial alignment. It also provides a guide to the maximum allowable transient thermal growth, before disengagement of the gear elements should be anticipated. In instances of large thermal transients, it may be necessary to modify the steady-state axial alignment to accommodate the transient thermal growth condition.

To put this in perspective, consider the hypothetical 40,000 hp (30,000 kW) compressor drive mentioned previously. Assume an external axial force is applied to the pinion by axial displacement of a typical flexible-disc type coupling,  $K = 5000$  lbf/in (875 kN/m). At steady-state operating conditions with reasonably loose alignment accuracy, less than 0.050 inch (1.3 mm) error, the axial coupling force would be 250 lbf (1100 N). For the gearset of this example, a 250 lbf axial mesh centering force would be generated by a helix transmitting 450 hp (335 kW). The mesh will remain centered if the transmitted power is greater than 1 percent of

normal load. If a typical diaphragm-type coupling was used ( $K = 20,000 \text{ lbf/in}$ ), the load necessary to keep the mesh centered could be closer to 3 or 4 percent of normal transmitted load.

INTRODUCTION TO EXAMPLES

Based on experiences such as those described in this paper, the authors believe the resulting nonuniform transmission of motion from a bound mesh can supply broad-spectrum angular or lateral excitation to the system. Experience has shown this can lead to excessive vibration by directly stimulating lateral displacement or through interaction of lateral and torsional vibration in the gearset (Hudson, 1992). Additionally, low bearing stiffness (such as encountered in a gearbox with pressure-dam bearings operating under light load) has been reported to increase the interaction between torsional and lateral response (Pennacchi and Vania, 2004). Finally, the combination of running on both the loaded and unloaded faces of the gears produces high relative variation in gear mesh stiffness. Variation in gear mesh stiffness has been discussed as a source of torsional excitation capable of producing noticeable lateral response (Iwatsubo, et al., 1984). If the axial force is extremely high, the wedging effect can cause tooth overload and failure, and thrust bearing wear can be accelerated.

The following examples illustrate practical problems that occurred because of thermal transients and axial misalignment. Four examples are described with emphasis on their vibration signatures. They highlight some common causes of excessive axial force in turbomachinery trains. Additionally, they provide lessons for designing trouble-free systems and for diagnosing problems. The first example will be discussed in considerable detail to illustrate the diagnostic process and illuminate how similar phenomena can be mistakenly blamed for the appearance of this subsynchronous vibration. The mechanics of the thermal transient growth and gear binding in Example 1 are presented in APPENDIX A. The second through fourth examples are included to present other train configurations that have experienced these phenomena and to illustrate some points not covered in the first example.

EXAMPLE 1—  
GAS TURBINE, GEARBOX,  
CENTRIFUGAL COMPRESSOR

This problem arose during a no-load string test of a 15,000 hp gas turbine, speed-increasing gearbox, and centrifugal compressor shown schematically in Figure 7. Maximum continuous speeds (MCOS) were 9300 rpm (155 Hz) at the turbine and 11,840 rpm (197 Hz) at the compressor. The original string test setup was “open-air,” the compressor had inlet and outlet silencers and absorbed only an estimated 250 hp. This train was very similar to an existing design that had performed well in field operation.

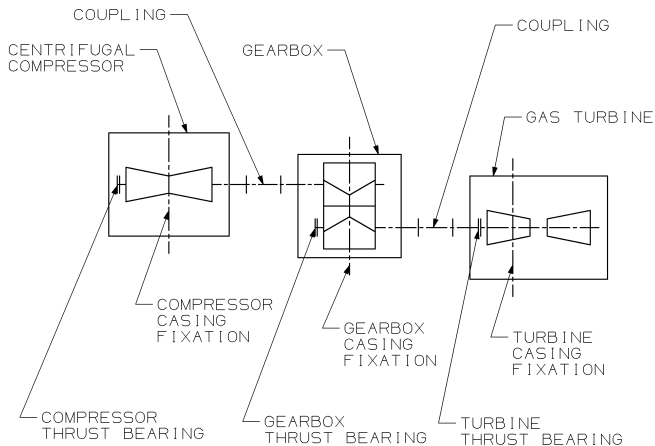


Figure 7. Layout of Gas Turbine, Gearbox, Centrifugal Compressor Train in Example 1.

As shown in Figure 8, string test results typically showed a variety of subsynchronous vibration (SSV) peaks in the gearbox low-speed (input) shaft displacements with most notable components near 30 to 40 and 70 to 80 Hz. The highest SSV peaks were approximately 0.0005 inch (0.013 mm) near 40 Hz. Amplitude at  $1\times$  was about 0.0005 inch (0.013 mm) and overall levels approached 0.002 inch (0.05 mm). Significant SSV appeared only after operating at MCOS for 12 to 30 minutes, disappearing after returning to idle speed. Only the gearbox low-speed shaft exhibited the SSV. All gearbox journal and thrust bearing temperatures were as expected. Review of relevant frequencies identified a small SSV peak near 35 Hz in the gearbox shop test. It also was noted that the predicted first torsional resonant frequency of the train was 41.8 Hz and the second was 75.5 Hz (refer to Figure 9). Preliminary diagnosis indicated axial alignment and journal bearing instability as possible contributors to the SSV problem.

POINT: 06 LSS DE VE-451X /135° Right  
MACHINE: Gearbox (LSS)  
From 28FEB2004 10:11:48.1 To 28FEB2004 12:07:27.3 Startup 10:42:00.5  
WINDOW: Hanning SPECTRAL LINES: 400 RESOLUTION: 2.5 Hertz

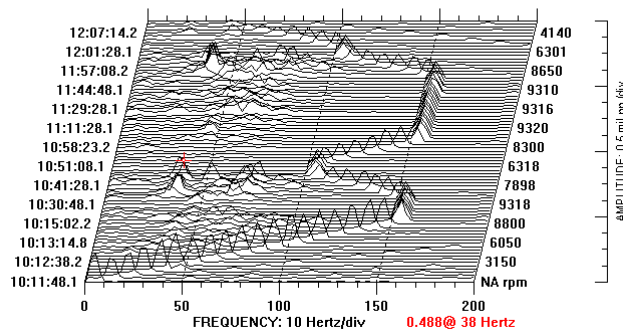


Figure 8. Radial Vibration of Gearbox Input Shaft During Typical String Test of Example 1.

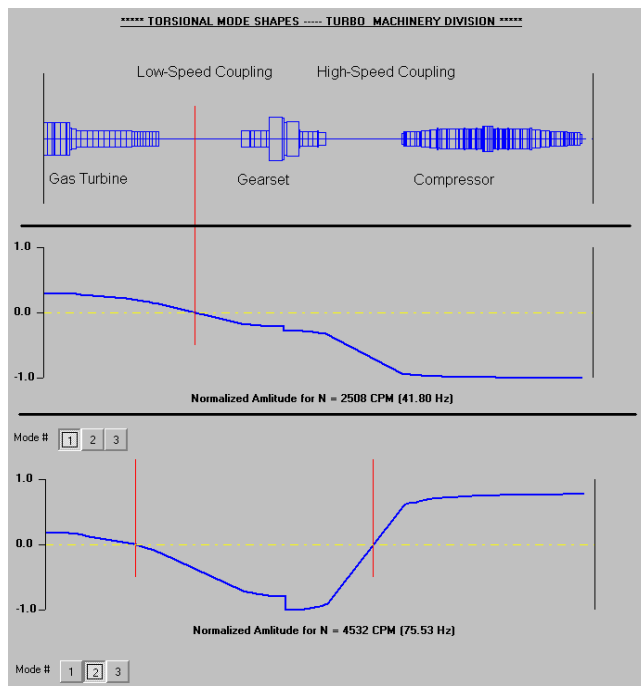


Figure 9. Torsional Model of Train from Example 1.

Diagnostic Run without Compressor

A diagnostic test was run with the compressor uncoupled from the gearbox output shaft. If the issue was journal bearing instability, the problem would get worse as the minimal 250 hp

compressor load was removed. Decreasing bearing load by decreasing torque should make the cylindrical bore, pressure-dam bearings in the gearbox less stable. If the issue was an axial alignment error, eliminating the compressor (and its thrust bearing) would eliminate the problem.

Performance of the unit during the uncoupled test showed the SSV had been eliminated (refer to Figure 10). The SSV peak just below 40 Hz in the original vibration spectrum was gone. A smaller peak appeared at 60 Hz, very close to the calculated 59.5 Hz first torsional resonance with the compressor removed from the train. This was a strong indication that there was some level of torsional/lateral interaction occurring in the train and that interaction was contributing to the SSV. This validated the theory that the source of the vibration was alignment related, most likely axial alignment.

POINT: 06 LSS DE VE-451X /135° Right  
MACHINE: Gearbox (LSS)  
From 03MAR2004 11:23:32.5 To 03MAR2004 12:05:22.5 Startup 11:49:47.5  
WINDOW: Hanning SPECTRAL LINES: 400 RESOLUTION: 1.25 Hertz

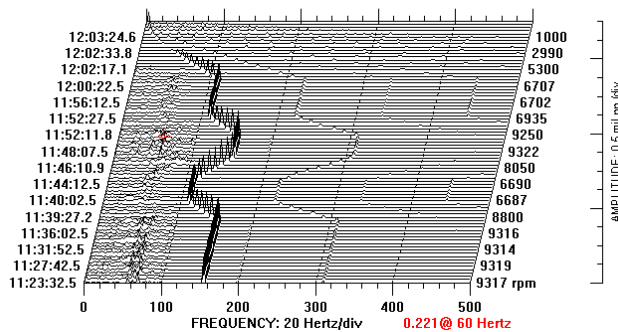


Figure 10. Radial Vibration During Diagnostic Test Run of Turbine and Gearbox Alone in Example 1.

#### Diagnostic Run with Decreased High-Speed Coupling Prestretch

An additional 0.020 inch (0.51 mm) shim was added to the high-speed coupling to decrease the prestretch to 0.018 inch. This did not solve the problem. Results at MCOS were similar to the initial runs, except that the SSV peaks were higher in amplitude and less vibration hash appeared between the peaks. SSV appeared approximately 10 to 15 minutes into the run, and discrete components reached 0.0011 inch (0.028 mm) levels. Frequencies were much more distinct at 39, 78, 116, and 155 Hz, all of which are related to the 155 Hz running speed. It appeared decreasing prestretch made vibration worse during shutdown. When the unit was manually tripped, the lateral vibration spiked to higher levels. This result focused attention on nonalignment issues.

#### Diagnostic Run with Light Torque Load

At this point attention turned to load. There was consensus that if sufficient torque load was placed on the train, the problems being experienced would be entirely eliminated, regardless of whether the problem was caused by axial misalignment or journal bearing instability. However, the only way to increase load on the train during the string test was to install an orifice on the compressor output, which was expected to add 250 hp additional load over the unthrottled configuration. This was done, but the resulting 500 hp load was not enough to make a significant difference, except that the time to onset of SSV was increased slightly.

#### Gearbox Modifications

Focus shifted to the gearbox journal bearing design as a means of decreasing vibration. Although rotordynamic analysis of the gearbox journal bearing design indicated there should be stable operation (even at zero load), it was decided that a different

bearing design could eliminate bearing stability as a possible factor and reduce vibration levels (Nicholas, et al., 1980). The reduced vibration level would also avoid machine protection trips and should provide a longer diagnostic run to help clarify the effect of other potential causes. The gear supplier developed a modified journal bearing design that was optimized for stability at no load and could be implemented by modifying the bearings that were in the machine. The low-speed (input) shaft journal bearings were removed from the gearbox, modified, and reinstalled.

At the same time the journal bearings were being modified, a provision was added to the gearbox for installing an axial proximity probe at the high-speed pinion. The intent was not to measure axial vibration of the pinion, but to monitor the axial position of the pinion and provide insight on axial alignment. It was expected the pinion axial probe would enable detection of gear mesh axial misalignment similar to Figure 5 or 6 if such a condition was present.

#### Diagnostic Run with Axial Probe on Pinion and Modified Journal Bearings

This run revealed that the subsynchronous vibration was correlated with axial misalignment of the gear mesh. Simultaneously monitoring the low-speed shaft radial vibration and pinion axial movement was the key to solving the problem. Verifying the pinion position and subsynchronous vibration levels changed in concert during the test illuminated the solution.

As shown in Figure 11, subsynchronous vibration appeared much the same as it had in previous runs. At about 8:42 the speed was increased from 9000 rpm to MCOS of 11,844 rpm. The lateral vibration probes showed that until 8:57:36 a clean subsynchronous spectrum was present with low amplitudes and no significant discrete components (light data in Figures 11 to 13). After that time, two significant SSV frequencies appear at 38 and 82 Hz (roughly corresponding to the first and second torsional resonances). This SSV remained consistent for 65 minutes (dark data in Figures 11 to 13) and then for a brief period the SSV presented varying frequencies. After that, a clean subsynchronous spectrum was present (second light data in Figures 11 to 13). During the deceleration at 11:00, the SSV reappeared momentarily, but subsided once the new speed of 9000 rpm was maintained. The modified (stiffer) bearings appeared to reduce subsynchronous discrete amplitudes and eliminated much of the nondiscrete SSV (noise or hash). However, they did not prevent the SSV from occurring.

POINT: LSS DE VE-451X /135° Right  
MACHINE: Gearbox (LSS)  
From 19MAR2004 08:34:46.4 To 19MAR2004 11:04:26.5 Startup 09:18:01.5  
WINDOW: Hanning SPECTRAL LINES: 400 RESOLUTION: 1.25 Hertz

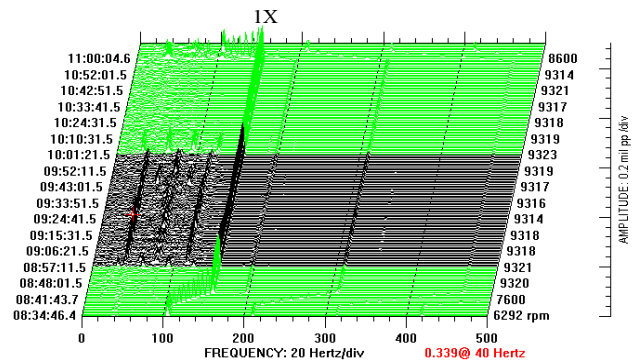


Figure 11. Radial Vibration after Installing Pinion Axial Probe in Example 1.

Figures 12 and 13 show high-speed pinion and low-speed gear axial positions. In these axial position plots 200 mV output voltage change corresponds to 0.001 inch (0.025 mm) axial position change (200 mV/mil). For example, during the period from 8:42



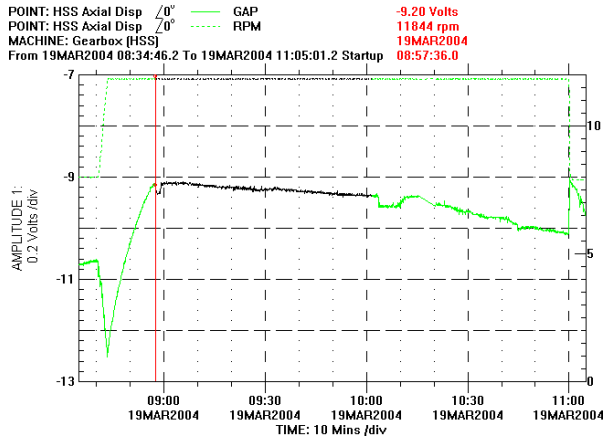


Figure 12. High-Speed Pinion Position Plot for Example 1.

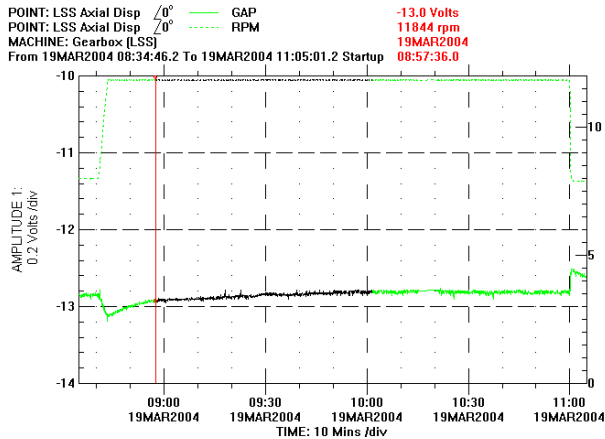


Figure 13. Low-Speed Gear Position Plot for Example 1.

until 8:56 the pinion probe voltage changed 3.4 volts. That represents a movement of 0.017 inch (0.43 mm). Not only was the pinion undergoing substantial axial displacement, comparing pinion and gear positions revealed that the pinion moved considerably further axially than the gear. This measurement verified the pinion and gear were not remaining axially centered on one another (similar to the condition depicted in Figures 5 and 6). Further evaluation of the data showed that the SSV began when the mesh became tightly bound (transition from light to dark data). Details of the evaluation are presented in APPENDIX A.

*Final Qualification Run with Increased Prestretch in High-Speed Coupling*

Based on results of the previous run, the coupling prestretch was increased an additional 0.040 inch (1 mm) to 0.058 inch (1.5 mm) and another run was completed. The modified bearings from the previous run were used. The gearbox was able to run through the thermal transients and be subjected to numerous speed cycles without the SSV appearing (refer to Figures 14 and 15). The axial probe indicated the pinion axial position leveled off smoothly at the maximum displacement, with no indication of mesh binding. Based on these results it was concluded that the problem was solved. The unit has subsequently entered service. No SSV has been detected during startup, steady-state, transient/load change, or shutdown.

**EXAMPLE 2—  
STEAM TURBINE, GEARBOX, GENERATOR**

Similar vibration behavior was experienced on a steam turbine-driven generator with a speed-reducing gearbox. In this train, the

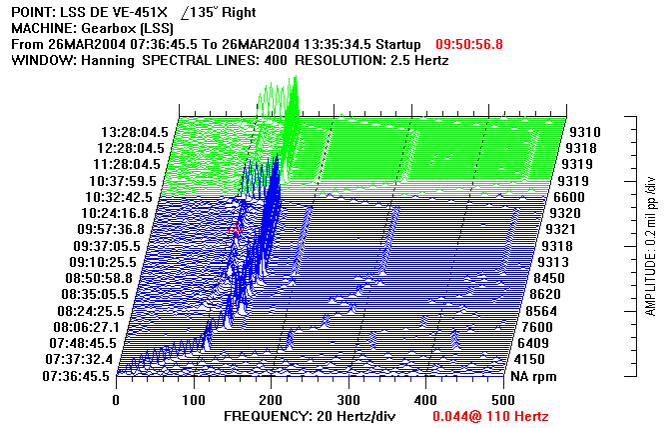


Figure 14. Vibration with Increased High-Speed Coupling Prestretch in Example 1.

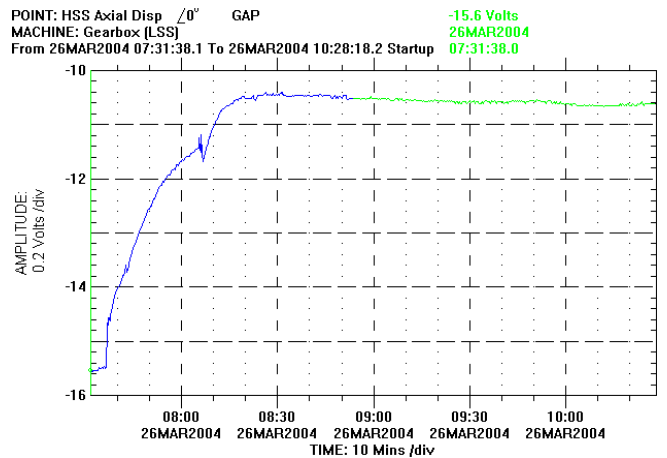


Figure 15. Pinion Axial Position Leveling Off Gradually in Example 1.

steam turbine is the driver. It is coupled to the high-speed pinion through a flexible element coupling. The low-speed shaft of the gearbox carried the thrust bearing and was connected to an electrical generator rotating at 1800 rpm. The train layout is shown in Figure 16.

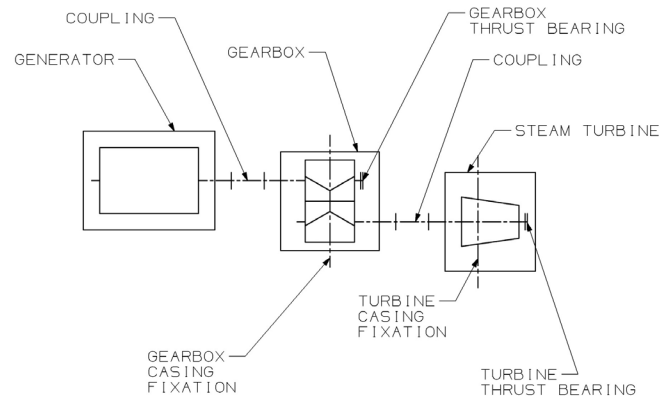


Figure 16. Layout of Turbine, Gear, Generator Train of Example 2.

During commissioning of the train, one of the checks performed was to unload the steam turbine at full speed by removing the generator load. This produces an unloaded condition in the gearbox. The sudden unloading of the steam turbine resulted in rapid cooling (and shortening) of the turbine rotor as the steam rate fell. During the first unloading cycle a subsynchronous vibration was measured

on the gearbox pinion shaft as shown in Figure 17 with no other excessive vibration appearing elsewhere in the train. The vibration appeared discretely at 750 cpm and 2100 cpm, with magnitude greater than the synchronous component. These SSV frequencies corresponded to the predicted first and second torsional natural frequencies of the train, 755 cpm and 2230 cpm, respectively.

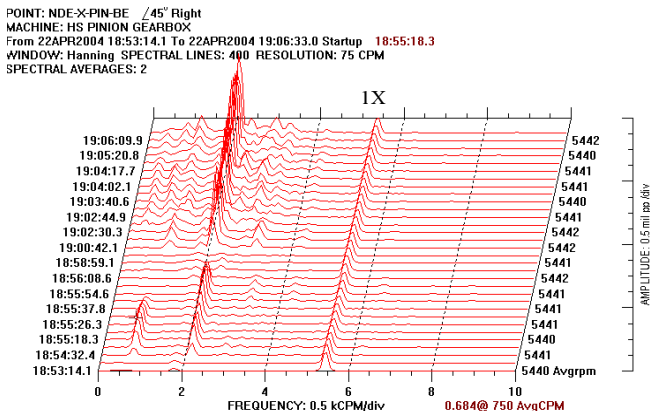


Figure 17. Radial Vibration of Pinion in Example 2.

*Diagnostic Run with Increased Coupling Prestretch*

The axial alignment of the train was modified after these characterization runs by increasing the prestretch of the high-speed coupling by 0.023 inch (0.6 mm). With this modification, the SSV continued.

It was hypothesized that the source of the vibration could be a thermal transient, causing axial displacement of the shaft end and shifting of the pinion to gear alignment. The sudden cooling of the steam turbine rotor had the potential to produce 0.10 inch (2.5 mm) of shaft-end movement. Unlike the situation described in Example 1 (when the growth of the compressor shaft tended to push the pinion shaft end toward the gear), in this example the motion of the turbine shaft end would be to pull the pinion shaft end away from the gearbox. In Examples 1 and 2, the axial force applied to the pinion is sufficient to overcome the mesh centering force of the double-helical gear set and drive the pinion out of axial alignment with the gear. With sufficient axial motion, the axial backlash of the gears would be consumed and the gearset would become “bound.”

*Diagnostic Run with Axial Probe on Pinion*

To verify the hypothesized behavior, an axial probe was installed in the gearbox to measure motion of the pinion. Figures 18 and 19 present similar behavior to that observed in Example 1. A sudden discontinuity in the pinion axial position [approximately 0.020 inch (0.5 mm) motion] trace corresponded to the rise of sub-synchronous vibration. This 0.020 inch (0.5 mm) displacement during operation agreed with the 0.018 inch (0.45 mm) of axial end play measured during installation checks.

*Diagnostic Run with Modified Thrust Bearing Clearance*

In order to remove the constraint on pinion motion imposed by the low-speed gear, the axial clearance of the thrust bearing was increased by 0.040 inch (1 mm) with the modification of the shim pack. The shims were intentionally changed to move the axial running position of the gear closer to the steam turbine. In effect, this decreased the prestretch of the high-speed coupling, decreased the pulling force on the pinion during the cooling transient (and increased the prestretch of the low-speed coupling). The behavior of the gearbox improved significantly. Limited vibration was seen during subsequent unloading and deceleration runs. The unit entered service to the satisfaction of the customer. Figure 20 shows the much cleaner waterfall spectrum. Prior to the changes, the 750 cpm component was equal to the 1× vibration level, while the 2100 cpm had been up to three times the 1× vibration level.

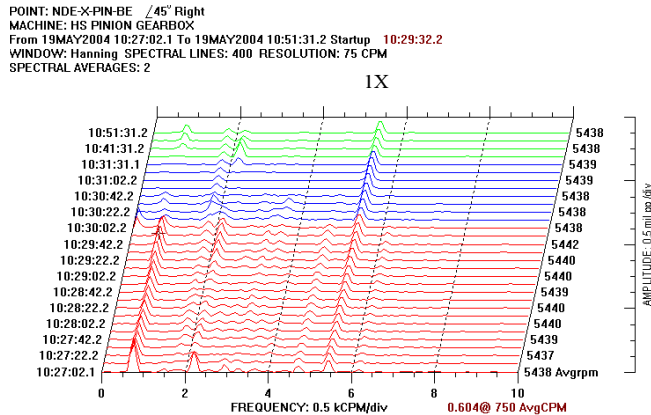


Figure 18. Radial Vibration after Installing Pinion Axial Probe in Example 2.

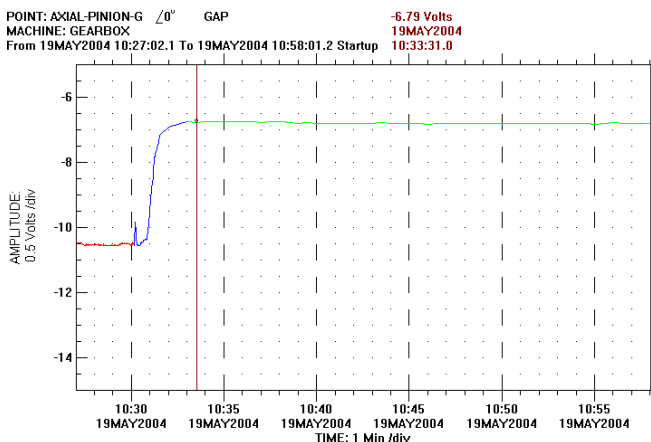


Figure 19. High-Speed Pinion Axial Position in Example 2.

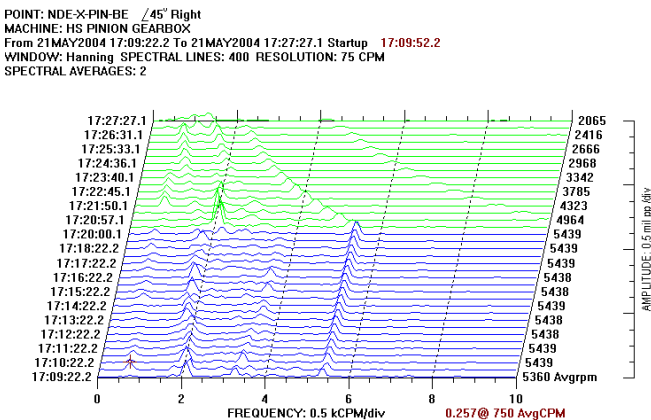


Figure 20. Radial Vibration after Increasing Thrust Bearing Clearance in Example 2.

EXAMPLE 3—  
STEAM TURBINE, GEARBOX, GENERATOR

Before the experiences described in Examples 1 and 2, a similar vibration behavior was encountered on another steam turbine-driven generator with a speed-reducing gearbox (layout shown in Figure 21). Although it was not understood at the time of the incident, it later became apparent that this was another instance of axial misalignment. As in Example 2, the steam turbine is the driver and is coupled to the high-speed pinion through a flexible element coupling. In this example, there were two separate but identical trains, and only one of the trains experienced the high vibration.

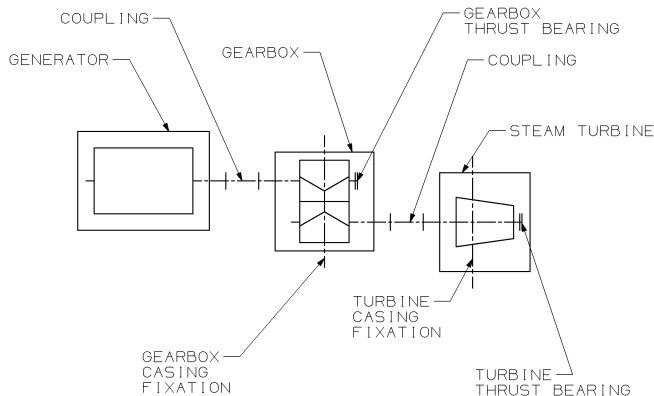


Figure 21. Layout of Turbine, Gear, Generator Train of Example 3.

During commissioning of one of the trains, the gear unit repeatedly tripped on high radial vibration of the pinion during startup. An examination of the pinion shaft vibration cascade plot (Figure 22) during startup revealed the main component of radial vibration to be subsynchronous, occurring at approximately 10 Hz once the train reached a generator speed of 950 rpm (full speed = 1800 rpm). It was later realized that this SSV frequency corresponds to the train's calculated first torsional natural frequency of 10 Hz.

MACHINE: Gearbox  
 From 12DEC2002 14:00:43 To 12DEC2002 14:41:03 Startup 1573 rpm  
 WINDOW: Hanning SPECTRAL LINES: 400 RESOLUTION: 1.25 Hertz

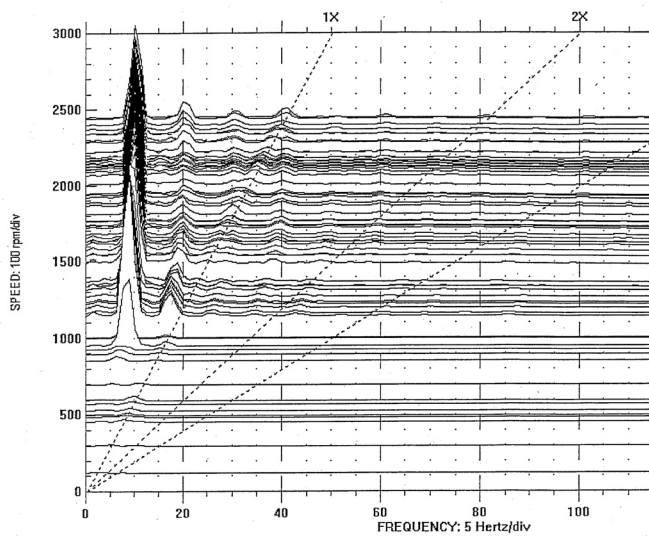


Figure 22. Radial Vibration of Pinion of Example 3.

At the time of the incident, the focus of the investigation centered on a journal bearing oil whirl. Accordingly, the pinion bearings were redesigned in an effort to suppress whirl. Before the installation of the modified bearings, an error was discovered on the installed prestretch of the high-speed coupling. The installed prestretch was 0.030 inch (0.8 mm) less than the calculated required value. This mistake was not made on the second train, which operated well and showed no signs of SSV. The decision was made to correct the prestretch by removing 0.030 inch (0.8 mm) of shim in the high-speed coupling at the same time the modified pinion bearings were being installed.

After the modifications, the pinion was able to reach full speed while showing no signs of SSV, and the train was commissioned successfully. An interesting point about this example is that there were two identical trains, but only one experienced a problem. The train with the correctly installed prestretch and original bearing design did not exhibit SSV.

EXAMPLE 4—  
 GAS TURBINE, GEARBOX, GENERATOR

This train contained a gas turbine driving a generator through a speed-reducing gearbox. The turbine was connected to the gearbox pinion by a diaphragm-type coupling. The gearbox low-speed shaft flange was bolted directly to the generator shaft flange without a coupling. As shown in Figure 23, there were thrust bearings at the nondrive end of the single-shaft gas turbine and on each side of the low-speed gear. The subsynchronous vibration occurred during commissioning while running at full speed and no load.

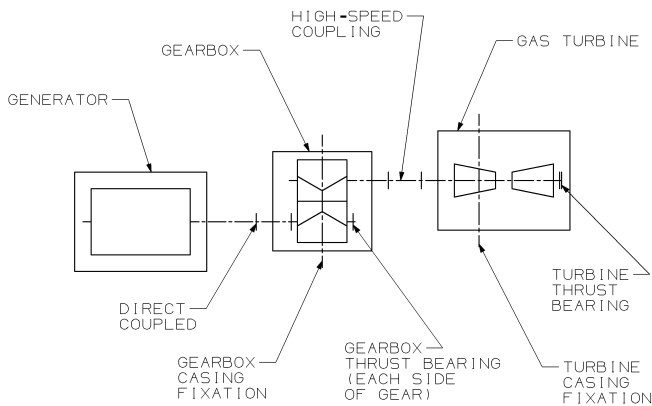


Figure 23. Layout of Gas Turbine, Gear, Generator Train of Example 4.

The train was started and brought to full speed at no load. During the first hour radial vibration was low. After running at no load about an hour, the high-speed pinion radial vibration began increasing and continued to increase during a period of several minutes until the machinery protection system tripped on high pinion radial vibration. This trip occurred shortly before the turbine was expected to complete its startup thermal transient. Limited vibration data were available from a condition monitoring system. The pinion radial vibration had a significant spectral component in the general vicinity of low-speed gear design rotating speed of 1800 cpm. Initially it was thought the pinion SSV was a forced response at the low-speed gear rotating frequency.

Following a test run to obtain better vibration data, it was determined the dominant SSV peak did not track gear rotating frequency. Further, the vibration could be observed in casing acceleration and pinion displacements. Figure 24 is a representative casing velocity spectrum showing frequencies involved. This sample was taken at rotating frequencies of 5109 cpm (85.1 Hz) at the turbine and 1800 cpm at the generator. The vibration frequency peak was fixed near 1875 cpm (31.2 Hz). Once again there was circumstantial evidence that torsional effects could be a factor because the predicted first torsional natural frequency was 1894 cpm, very close to the response frequency.

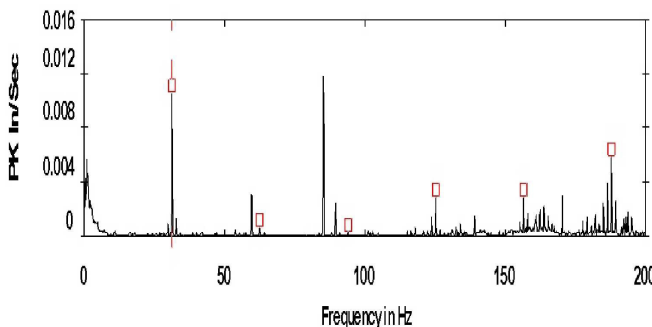


Figure 24. Original Vibration Spectrum for Example 4.



Axial alignment of the turbine to the gearbox pinion was reviewed. It was found that coupling axial thermal growth was not included in the original high-speed coupling prestretch calculation. The new analysis indicated that before steady-state conditions were reached there would be enough thermal growth in the turbine, coupling, and pinion to push the pinion away from the turbine into a bound condition as shown in Figure 6. Further, the growth was sufficient to push the low speed shaft through its thrust bearing clearance. Once the mesh was bound and the gear was pushed against its thrust bearing the remaining thermal growth had to be absorbed by axial deflection of the high-speed coupling. The relatively high coupling axial stiffness enabled even a small amount of coupling deflection to create sufficient force to bind the mesh.

#### *Diagnostic Run with Increased Coupling Prestretch*

A test run was made with high-speed coupling prestretch increased from 0.110 to 0.130 inch (2.8 to 3.3 mm) and with an axial position probe installed at the high-speed pinion. This change was not sufficient to solve the problem. However, the axial probe confirmed that the pinion was moving axially as predicted. The machine appeared to run acceptably on one helix, but the SSV picked up when the pinion reached its maximum axial displacement relative to the gear. Further increase of coupling prestretch was considered undesirable because of a turbine shaft axial excursion of 0.16 inch (4.1 mm) away from the gearbox early in the run. Thus another means of reducing axial misalignment was sought.

#### *Diagnostic Run with Modified Thrust Bearing Clearance*

Gearbox thrust bearing clearance was increased for the next run. The resulting combination of gear mesh and thrust-bearing clearance in the gearbox allowed  $\pm 0.06$  inch (1.5 mm) of pinion axial motion. Based on the axial alignment review, this was believed to be sufficient to absorb the thermal transients. Following the modification, the machinery protection system did not trip. Furthermore, the axial probes showed both the pinion and low-speed gear were pushed axially away from the turbine. Vibration began to increase at roughly the same time after the start of the run as it had previously. However, before the vibration reached an undesirable level, the pinion and gear were both observed to axially shift away from the turbine and the vibration decreased. This axial shift was possible only after the gearbox thrust bearing clearance was increased. The shift allowed the pinion to move away from the turbine without tightly binding the mesh. This was additional evidence that transient axial misalignment had caused the SSV problem. The startup trip did not reappear in subsequent runs either with or without load. The modification permitted the commissioning process to continue.

### DIAGNOSIS OF AXIAL ALIGNMENT PROBLEMS

A few main points relevant to diagnosing axial alignment problems are summarized here. Although some may not be practical in a particular situation, it would be prudent to consider these checks if the usual diagnostic process does not identify the problem. At a minimum, steps such as reviewing axial alignment and checking predicted torsional frequencies should be taken. If an axial alignment issue is found, the options described in the examples and in the following section should be helpful.

- Review axial alignment calculations, installation results, and related factors. This includes thrust bearing clearances, gearset backlash, coupling stiffness, coupling prestretch, and distance between shafts. In particular, ensure coupling axial thermal growth is included in axial alignment calculations.
- Review predicted torsional natural frequencies for a match with observed response frequencies. As seen in the examples, there is often a correlation between measured gearbox response frequencies and predicted torsional frequencies. Spectral data with good resolution taken during the vibration event are required.
- Evaluate the possibility of oil whirl or oil whip if fixed geometry bearings are used. These are complicated phenomena beyond the scope of this paper, but for most gearboxes a few basic observations using a waterfall plot are sufficient for a first evaluation. Oil whirl usually can be ruled out if the frequency of shaft motion does not remain at about 40 to 45 percent of running speed as speed increases. On a waterfall plot oil whip looks like oil whirl initially but instead of continuing to track running speed it locks onto a resonant frequency and remains at that frequency as speed increases.
- Monitor pinion and gear relative axial positions in conjunction with vibration during the test run. If there is no existing axial probe provision, one can be added. In Examples 1, 2, and 4, an eddy-current proximity probe at the pinion allowed direct verification of pinion axial movement. It is not necessary to have a high-quality axial probe target area since the purpose is to measure relatively large rotor movements using a direct current (DC) signal. Pinion and gear motion should be compared to the axial backlash in the gearset. Timing of these motions can be compared with changes in vibration.
- Verify coupling (or enclosure) temperature rise and compare to the expected value.
- Machinery protection system trips can hinder diagnosis. The equipment suppliers involved can be consulted for ways to reduce response or for other options to prevent unnecessary trips that hinder diagnosis. For instance, in Example 1 a temporary gearbox bearing change reduced response during the diagnostic process.
- Perform test runs with varied loading. Lighter load reduces the mesh centering force and may make the problem worse. Heavier load increases mesh centering force and makes the gearset more resistant to external axial forces.
- Perform a test run with the driven equipment uncoupled. In addition to removing load, this can remove one source of axial force on the gearset. This test is most productive if the gearbox output shaft does not have a thrust bearing.

### DESIGN AND ANALYSIS TO PREVENT AXIAL ALIGNMENT PROBLEMS

The axial alignment of a turbomachinery train including a double-helical gear unit should address all operating modes of the train. This requires consideration of both steady-state equilibrium thermal growth and transient thermal growth during startup, shutdown, or unloading cycles that may be encountered in field operation. Test conditions must also be considered, particularly if testing includes running at essentially no torque load. If properly applied at the design stage the following observations should help prevent future problems. They may also be helpful in correcting problems in existing trains.

- Coupling prestretch can help accommodate thermal growth in the train. However, care must be taken to ensure the flexible elements of the coupling will not be damaged. There may be axial position excursions in both directions during startup thermal transients. A compromise coupling prestretch value may be required to accommodate both transient and steady-state axial alignment conditions.
- Coupling thermal growth should be included in prestretch calculations, as well as thermal movements of the shaft ends and casings of connected machines.
- Coupling enclosures should be properly designed to prevent excessive coupling heating and thermal growth.
- Coupling flexible element axial stiffness can be lowered to accommodate more axial growth without generating large axial forces.

- Thermal growth analysis of involved components must include consideration of maximum and minimum transient thermal states, such as when rotor components are hot and casings are cool. This will allow a comprehensive axial alignment chart to be produced.
- A thrust bearing can be situated in the gearbox on the shaft to which the largest external force is applied. This can prevent the axial force from reaching the mesh. However, the thrust bearing must be capable of absorbing the axial force. It should be kept in mind that purchasing specifications often dictate gearbox thrust bearing location. For example, API 613, Fifth Edition (2003), states that a double-helical gearbox shall have a thrust bearing on the low-speed shaft unless specified otherwise by the purchaser.
- The gearbox thrust bearing clearance can be increased. The gearset can even be allowed to float axially without a thrust bearing to absorb motion of connected equipment. However, this option may not be possible for some train layouts. Also, there can still be a problem if the connected machines can exert axial force on both gearbox shafts.
- Increased backlash can accommodate more mesh axial offset, but excessive backlash can reduce the load capacity of the gearing by excessively thinning the teeth. It can also increase the severity of transient torsional vibration in some trains.
- Casing fixation locations of connected machines can be altered to reduce shaft end excursions.
- Changes of startup sequences or other thermal management schemes can be considered.

## SUMMARY

A double-helical gearbox relies on transmitted torque to generate mesh axial forces that hold the pinion centered on the gear. If an external axial force is larger than the mesh force, it can push the pinion and gear off center with one another. This is most likely to occur in unloaded trains such as a generator drive prior to application of electrical load or a compressor drive in a no-load string test. The external force is most commonly caused by axial misalignment of the connected equipment. This misalignment may be due to an error in design or installation, or it may be a temporary effect caused by transient thermal growth.

Axial alignment errors and thermal transients in turbomachinery trains can produce axial displacements, which must be absorbed by the coupling flexible elements. If the axial displacements are large, and the flexible element stiffness is high, the resulting forces and axial motion of the pinion relative to the gear can be sufficient to consume all the axial clearance in the gearset and bind the mesh, essentially producing a gearset running without backlash.

Four field examples have been presented where axially bound gearsets have excited subsynchronous torsional resonances. The mechanical coupling of torsional and lateral motion in a gearbox results in the torsional vibration producing a lateral response. Depending on the stiffness of the bearings, varying levels of lateral response are measured, but as shown in the examples these vibrations can be sufficient to trip the machinery protection system.

Several diagnostic checks are available to help distinguish axial alignment problems from other sources of vibration. They range from the relatively easy tasks of reviewing axial alignment and predicted torsional frequencies to more difficult and expensive checks such as special test runs. The diagnostic value of an axial probe on the pinion has been well demonstrated. In Examples 1, 2, and 4, this probe allowed direct verification of the phenomena. The verification allowed the involved parties to agree on a solution that would allow successful completion of the testing or installation of the equipment without compromising the operational performance of the machinery.

Fortunately, options are available at the design stage to mitigate the effects of axial thermal growth. Careful axial alignment analysis and judicious use of design parameters such as thrust

bearing location, thrust bearing clearance, gearset backlash, and coupling prestretch can help prevent axial alignment problems. System designers, gear unit suppliers, and others such as coupling suppliers should work together to ensure that the equipment will operate satisfactorily.

Ultimately, concerns about transient thermal growth and subsequent impact on operating alignment between gear elements are a system-level issue. A comprehensive analysis should be performed to ensure the design respects the constraints of each system component. Good communication and cooperation at the design stage are crucial, particularly if there are large thermal effects or other special circumstances.

## APPENDIX A— SUPPLEMENT TO EXAMPLE 1

### *Discussion of Physical Events During Diagnostic Run with Axial Probe on Pinion*

The following paragraphs provide a physical interpretation of the problem deduced from position measurements, vibration data, and mechanics of the machine components. Refer to the section titled “*Diagnostic Run with Axial Probe on Pinion.*” Figure A-1 depicts the location of the axial probe on the pinion blind end, access panel.

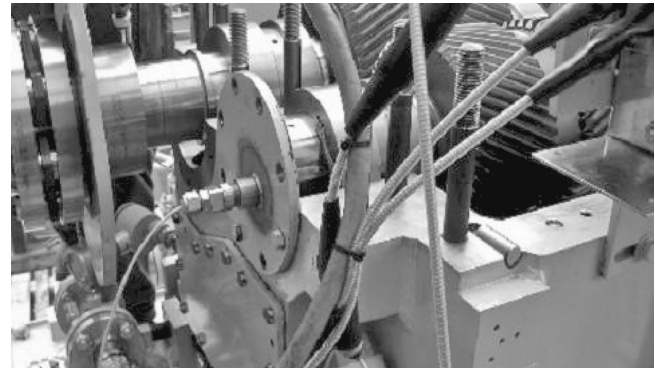


Figure A-1. Photograph of the Axial Probe Installation in Example 1.

During axial alignment of the train, the bull gear was centered in its thrust bearing clearance and the pinion was centered relative to the gear. At that point all components were at ambient temperature and there was a small prestretch in the coupling flex elements [nominally 0.018 inch (0.5 mm)].

The train was started and idled as usual as the equipment began to heat up. At 8:42 the compressor speed was increased from 9000 to 11,844 rpm. This caused two things to happen. First, as speed increased, the torque absorbed by the compressor increased slightly and so did the mesh centering force. This caused the pinion to move axially, changing coupling displacement to maintain equilibrium between the mesh centering force and coupling compression force. This is shown in Figure 12 as a downward movement of the position trace of about 1 V, indicating the pinion moved about 0.005 inch (0.13 mm) toward the compressor (the probes provide 200 mV/mil displacement). Because higher torque (and therefore an increased mesh centering force) caused the pinion to move closer to the compressor, it can be inferred that thermal growth prior to 8:42 had pushed the pinion away from the compressor and moved it off center relative to the gear. Figure 13 shows that the low-speed gear simultaneously moved about 0.0015 inch (0.038 mm) away from the compressor. Because the axial probe on the low-speed gear was oriented in the opposite direction, downward motion of the gear position voltage indicates motion away from the compressor.

The second occurrence at 8:42 was the temperature of the compressor rotor and case began rising substantially again. As the

compressor came to MCOS, the various parts of the high-speed shaft line began to quickly heat and grow axially. The thermally massive case did not heat up as fast, and took longer to grow axially. The net result was that the compressor shaft end moved axially toward the gearbox. The thermal differential growth of the high-speed rotor string from the mesh center to the compressor thrust bearing was 0.066 inch (1.7 mm) (0.066 inch = 0.042 inch compressor shaft + 0.015 inch coupling + 0.009 pinion shaft). Furthermore, the low-speed gear was undergoing a similar thermal transient that was pushing the gear away from the gas turbine and against the gear thrust bearing. This also served to compress the high-speed coupling and increase the axial load on the pinion. Normally (i.e., when under load), the torque transferred and the double-helix centering force would have kept the two gear elements in axial alignment, and the transient axial growth would have been absorbed by the flexible elements of the coupling. But that did not happen in this test since torque load was near zero.

Recalling the discussion related to Figures 5 and 6, under light-load conditions, the maximum mesh axial centering force was much less than at normal operating torque, approximately 100 lbf (445 N) in this instance. Based on the axial stiffness of the coupling flex elements,  $K = 4000$  lbf/in (700 kN/m), only 0.025 inch (0.6 mm) of displacement was needed to produce in excess of 100 lbf (445 N). The calculated 0.066 inch (1.7 mm) thermal growth and the 0.018 inch (0.5 mm) prestretch of the coupling result in 0.048 inch (1.2 mm) of compression in the flex element, which should produce 192 lbf (855 N) axial load if the mesh remained centered. This was sufficient to slide the pinion axially along only one helix while the teeth of the opposite helix would not be making contact (as shown in Figure 5).

From 8:42 to 8:57 the pinion position could be seen moving smoothly away from the compressor as shown by the steady rise in the pinion position voltage in Figure 12. During that time, speed and torque were constant and the pinion was moving axially along with the compressor shaft end. Because the pinion was moving axially relative to the gear, it was clearly running on one helix as shown in Figure 5. Note that there was practically no SSV at this time, indicating that the gearset can run smoothly on one helix.

At 8:57:36 (where the data transition from light to dark), the moment significant SSV first appeared as shown in Figure 11, the pinion axial motion abruptly stopped as shown by the sharp discontinuity in Figure 12. This suggests that an obstacle had presented itself to restrict that motion. Based on distance traveled and the fact that there were no other obstructions to stop the pinion, it was clear that the pinion stopped moving axially because it reached a bound condition with the gear (as shown in Figure 6).

For about an hour after 8:57:36 the data show the mesh was bound tightly. When the pinion stopped moving axially, the compressor thermal transient had not been completed and the compressor shaft end position had not reached its full excursion toward the gearbox. For the next hour the pinion axial position was very nearly constant even though the compressor shaft end would have still been moving, initially growing toward the gearbox, then pulling away as compressor case growth caught up with the rotor. Once the pinion reached the end of its travel in the mesh clearance, any additional compressor shaft growth had to be accommodated by increasing axial compression of the high-speed coupling. Therefore during the hour that the pinion did not move, it must have been forced tightly in the mesh. The SSV continued undiminished throughout this hour period.

After one hour, corresponding to the time when the SSV began to change and the data transition from dark to light in Figures 11 to 13, the pinion began to return to its initial axial position. This change corresponds to the compressor casing warming and pulling the compressor shaft end away from the gearbox. At thermal equilibrium, the compressor case provides 0.030 mil (0.8 mm) of axial growth in the opposite direction from the initial shaft growth. Even though the compressor shaft had begun moving back away from the gearbox before the end of the hour, the pinion did not move

axially relative to the gear until the coupling compression decreased sufficiently for the coupling axial force to reach equilibrium with the axial mesh force. When this equilibrium was reached the pinion began moving with the compressor shaft end as it moved back toward the compressor. At this point the pinion was becoming unbound and returning to the condition shown in Figure 5. Shortly after the pinion began to move back toward the compressor, the discrete SSV components vanished, leaving the subsynchronous spectrum clean.

When speed was decreased from 11,840 to 9000 rpm (at 11:00), the pinion position moved abruptly away from the compressor, momentarily returning back to the same axial position where it stopped moving axially during initial startup. This happened because the speed decrease reduced the torque transmitted across the gearset and the corresponding gear mesh centering force, allowing the remaining coupling axial force to push the pinion back to its bound position. During this period, SSV briefly reappeared and then subsided.

It is important to note that numerous additional runs and stop cycles had produced many data sets for review. Careful observation of the shutdown behavior indicated that the vibration spikes (at 40 and 80 Hz) were not tracking with the  $1\times$  speed as the train decreased in speed. Instead, as train speed decreased, the 40 and 80 Hz components remained at a fixed frequency as shown in several of the preceding vibration plots. This behavior is not consistent with an oil whirl. However, it does appear consistent with an excitation of the first and second torsional frequencies.

## REFERENCES

- API Standard 613, 2003, "Special-Purpose Gear Units for Petroleum, Chemical and Gas Industry Services," Fifth Edition, American Petroleum Institute, Washington, D.C.
- Carter, D. R., Garvey, M., and Corcoran, J. P., 1994, "The Baffling and Temperature Prediction of Coupling Enclosures," *Proceedings of the Twenty-Third Turbomachinery Symposium*, Turbomachinery Laboratory, Texas A&M University, College Station, Texas, pp. 115-123.
- Drago, R. J., 1988, *Fundamentals of Gear Design*, Boston, Massachusetts: Butterworth-Heinemann.
- Dudley, D. W., 1984, *Handbook of Practical Gear Design*, New York, New York: McGraw-Hill.
- Dudley's Gear Handbook, Second Edition*, 1991, Townsend, D. P., Editor, New York, New York: McGraw-Hill.
- Hudson, J. H., 1992, "Lateral Vibration Created by Torsional Coupling of a Centrifugal Compressor System Driven by a Current Source Drive for a Variable Speed Induction Motor," *Proceedings of the Twenty-First Turbomachinery Symposium*, Turbomachinery Laboratory, Texas A&M University, College Station, Texas, pp. 113-123.
- Iwatsubo, T., Arii, S., and Kawai, R., 1984, "The Coupled Lateral Torsional Vibration of a Geared Rotor System," *Proceedings of the Third International Conference on Vibrations in Rotating Machinery*, IMechE, C265, pp. 59-66.
- Mancuso, J., July 24, 1986, "Disc vs Diaphragm Couplings," *Machine Design*, pp. 95-98.
- Nicholas, J. C., Barrett, L. E., and Leader, M. E., 1980, "Experimental-Theoretical Comparison of Instability Onset Speeds for a Three Mass Rotor Supported by Step Journal Bearings," *Journal of Mechanical Design*, ASME, 102, pp. 344-351.
- Pennacchi, P. and Vania, A., 2004, "Model-Based Analysis of Torsional and Transverse Vibrations of Geared Rotating Machines," *Proceedings of the Eighth International Conference on Vibrations in Rotating Machinery*, ImechE, C623, pp. 251-260.

Zirkelback, C., 1979, "Couplings—A User's Point of View," *Proceedings of the Eighth Turbomachinery Symposium*, Turbomachinery Laboratory, Texas A&M University, College Station, Texas, pp. 77-81.

#### BIBLIOGRAPHY

Eshleman, R. L., 1997, "Torsional Vibration of Machine Systems," *Proceedings of the Sixth Turbomachinery Symposium*, Turbomachinery Laboratory, Texas A&M University, College Station, Texas, pp. 13-22.

#### ACKNOWLEDGEMENTS

The authors would like to thank the management of Dresser-Rand, Lufkin, and Petronas Carigali for their support in publishing this paper. The authors also would like to acknowledge the support of Mr. Ed Turner (Dresser-Rand) and Mr. Craig Kujawa (Solar Turbines) in collecting data, Mr. Rob Kunselman (Dresser-Rand) for creating graphics, and Mr. Richard Pilsbury (Dresser-Rand) and Mr. Mark Winthrop (Lufkin) for assisting in the modifications required to perform the diagnostic testing.